FIN PROFILE OPTIMIZATION FOR MAXIMUM HEAT TRANSFER ACROSS AN ENCLOSURE FILLED WITH A FLUID

By

MIAO HUANG

A THESIS PRESENTED TO THE GRADUATE SCHOOL
OF THE UNIVERSITY OF FLORIDA IN PARTIAL FULFILLMENT
OF THE REQUIREMENTS FOR THE DEGREE OF
MASTER OF SCIENCE

UNIVERSITY OF FLORIDA

2017

To my parents

ACKNOWLEDGMENTS

Dr. S. Moussa Mirehei advised this research. I would like to thank him, for that and serving on the thesis committee. I would also like to thank Dr. S.A. Sherif for serving as the committee chair, and Dr. Chung, for serving on the thesis committee. I thank Yiqing Chen for helping me.

TABLE OF CONTENTS

page

LIST OF FIGURES

Figure page

NOMENCLATURE

c	fluid specific heat (J/kgK)
c_F	FLUENT fluid specific heat (J/kgK)
c_s	solid specific heat (J/kgK)
$c_{s,F}$	FLUENT solid specific heat (J/kgK)
g	gravitational acceleration (m/s^2)
g_F	FLUENT gravitational acceleration (m/s^2)
h	heat transfer coefficient (W/m^2K)
H	enclosure height (m)
k	fluid thermal conductivity(W/mK)
k_F	FLUENT fluid thermal conductivity(W/mK)
k_s	solid thermal conductivity(W/mK)
$k_{s,F}$	FLUENT solid thermal conductivity(W/mK)
L	enclosure width (m)
M	normal direction non-dimensional coordinate
n	normal direction coordinate
p	pressure(pa)
P	non-dimensional pressure
p_1	dimensional distance from top of the fin to top of the enclosure (m)
P_1	non-dimensional distance from top of the fin to top of the enclosure
p_2	dimensional distance from top of the fin to bottom of the fin (m)
P_2	non-dimensional distance from top of the fin to bottom of the fin
Pr	Prandtl number

q heat flow of fluid (W)

q_s heat flow of solid (W)

Ra Rayleigh number

S enclosure aspect ratio

T temperature of fluid (K)

T_s temperature of solid (K)

T_h left wall temperature (K)

T_c right wall temperature (K)

u horizontal velocity component(m/s)

U non-dimensional horizontal velocity component

v vertical velocity component(m/s)

V non-dimensional vertical velocity component

x horizontal coordinate

X non-dimensional horizontal coordinate

y vertical coordinate

Y non-dimensional vertical coordinate

α fluid thermal diffusivity(m^2/s)

α_s solid thermal diffusivity(m^2/s)

β isobaric coefficient of volumetric thermal expansion$(1/K)$

β_F FLUENT isobaric coefficient of volumetric thermal expansion$(1/K)$

θ Non-dimensional fluid temperature

θ_s Non-dimensional solid temperature

κ solid-to-fluid thermal conductivity ratio

μ_F	FLUENT dynamic viscosity (kg/ms)
μ	dynamic viscosity(kg/ms)
v	kinematic viscosity(m^2/s)
ρ	fluid density(kg/m^3)
ρ_F	FLUENT fluid density(kg/m^3)
ρ_s	solid density(kg/m^3)
$\rho_{s,F}$	FLUENT solid density(kg/m^3)
σ	solid-to-fluid volumetric heat capacity ratio

Abstract of Thesis Presented to the Graduate School
of the University of Florida in Partial Fulfillment of the
Requirements for the Master of Science

FIN PROFILE OPTIMIZATION FOR MAXIMUM HEAT TRANSFER ACROSS AN ENCLOSURE FILLED WITH A FLUID

By

Miao Huang

December 2017

Chair: S.A. Sherif
Major: Mechanical Engineering

The problem of cooling of electronics has been extensively studied in the last few decades. Recently, studies considering heterogeneous enclosures filled with a fluid and solid bodies heated from the side, in which an isothermal hot wall at a higher temperature, an isothermal cold wall at a lower temperature, and adiabatic horizontal surfaces were considered, were reported. Although significant progress has been made in understanding the processes involved in heating and cooling of such containers, the effect of extended surfaces (fins) and their profile on heat transfer from the containers has not been considered. In this thesis, the effect of an extended hot wall surface on the cooling process is studied, and the fin profile with maximum cooling effect is determined using genetic algorithms. The left and right walls of the enclosure are considered isothermal and at T_h and T_c ($T_h > T_c$), respectively, while the top and bottom surfaces are considered adiabatic. The porosity (fluid volume fraction) of the enclosure is set at 0.84, and the Rayleigh and Prandtl numbers are set at 10^7 and 1, respectively. Optimization is performed for fins with rectangular profile. The heat transfer process is monitored in terms of total heat flux at the cold surface. Results are reported in terms of

fin profiles with the associated total heat flux and instantaneous isotherms and streamlines. Findings elucidate the effect of changes in the fin profile on heating and cooling of containers by natural convection.

CHAPTER 1
INTRODUCTION AND LITERATURE REVIEW

Methods of Analysis for Enclosure with a Solid and a Fluid

Cooling of solid parts distributed in an enclosure filled with fluid is relevant in a lot of engineering applications, especially cooling of electronics. Commonly the enclosure consists of a solid and a fluid. One way to calculate the heat transfer performance of such an enclosure is to consider it as a porous medium. The problem can be solved by the “porous-continuum” approach [1, 2]. In this approach, there are only conservation equations of a porous medium instead of separate conservation equations of the fluid and the solid. These equations can be derived by averaging the conservation equations of mass of fluid and solid, applying the volume theorem [3], and applying the conservation of energy between the fluid and the solid. A representative elementary volume needs to be determined in this case. However a representative elementary volume may become invalid when the solid portion is relatively large which would eventually make the porous-continuum approach invalid. For this reason, another approach is chosen which uses separate conservation equations of the solid and fluid. At the interface of the fluid and solid, an appropriate compatibility condition is applied. Although significant progress has been made in understanding the processes involved in heating and cooling of such containers and numerical simulations of heat transfer in enclosures employing this approach can be accurate [4-13], the effect of extended surfaces (fins) and their profile on heat transfer from the containers has not been considered. Periodic horizontal heating of enclosed disconnected solid bodies saturated with a fluid has been investigated by Mirehei et al. [14] and simulations and analyses of

natural convection inside heterogeneous containers heated by solar radiation has been reported by Mirehei [15].

Effects from Geometries and Properties of Fins on Heat Transfer Performance

Huang et al. [16] studied the dynamic characteristics of rectangular fin arrays. Gravity is taken into consideration and downward flow is proven to have negative effects on fins because of the thicker boundary layer. Heat transfer performance will increase with the fin length. Harahap et al. [17] pointed out that the orientation of the length of the fins parallel to the shorter side of the base plate would result in higher heat transfer efficiency than what would have been obtained using the longer side. Heat transfer efficiency drops drastically if the fin base area is smaller than the optimal area. Al-Doori et al. [18] showed that perforations positively affect the heat transfer efficiency. Also, as the diameter and number of perforations increase the heat transfer performance would increase. Dannelley [19] showed for most fractal geometries that they can enhance the heat transfer per unit mass without too much increase in the mass compared to traditional fin shapes. And for extended surfaces certain fractal geometries can increase the heat transfer per unit mass and thus reduce the mass of the fin, especially under natural convection conditions. Azarkish et al. [20] studied the improvement of heat transfer employing a number of fin arrays and selecting the right fin geometry. Results indicated that changing the fin geometry does not result in any change in the number of optimal fin arrays. For one-dimensional heat transfer, an optimized fin geometry is better than a non-optimized or conventional fin geometry. d. If two-dimensional heat transfer is considered, the fin geometry starts to play a role. Bobaru et al. [21] studied the relation between optimal fin shapes and the thermal conductivity of the material. High conductivity results in a sharp-pointed optimal

geometry. Low conductivity materials will result in a blunt and wide base geometry. Kang et al. [22] focused on trapezoidal fins. As the ratio of the convection characteristic number increases or the fin base radius decreases, the optimal heat transfer rate will increase. Hamadneh et al. [23] studied different conventional fin shapes including square, rectangle, circle and elliptical fins. Their results showed that a square is the worst shape while a rectangle is the best one from the standpoint of the rate of entropy generation.

Use of Genetic Algorithms in Heat Transfer

Genetic algorithm is a method to solve optimization problems. It can be applied in a multi-objective or a single objective optimization situation. This algorithm is similar to the natural selection process in nature. It will generate a generation with random individuals for the model which needs to be optimized. A fitness function will be applied on each individual to evaluate how good the individual is. Then individuals in this generation may crossover or mutate by chance. These two behaviors will either produce new individuals or change the existing individuals. The next generation will be selected by choosing the best individuals from the most recent generation according to the value of their fitness function. The crossover, mutation and selection process will repeat for iterations until stopping conditions are met. As the mutation probability increases, the optimization will be more random so low mutation probability is recommended. Low crossover probability will make the generation more stable and will get the results faster but less accurate. High crossover probability (>0.9) is also recommended [30]. Common stopping conditions are the limits on the number of iterations and/or stall

generation. The limit on the number of iterations refers to the stopping the algorithm after a certain number of iterations have been executed. The stall generation limit refers to the case when the fitness function value of the best individual in the current generation does not change by a significant extent after a certain number of generations has been created. This limit is called the convergence stability percentage in ANSYS and is chosen as the convergence criterion for this work.

Hajabdollahi et al. [24] used genetic algorithms to optimize a one dimensional pin fin. They used Bezier [24] curves to describe the fin profile. Total heat transfer and fin efficiency are the two objects. Their results identified the optimum fin shapes and their heat transfer performance. Higher dimensional cases are not involved. In this thesis two-dimensional cases will be analyzed. Wang and Wang [25] optimized the conical fin by dividing it into finite elements and making every element transfer the maximum heat flux. Fin effectiveness was not considered and the heat transfer rate was the only object. Results can be generated faster and better by a step calculation method than by traditional genetic algorithms. Najafi et al. [26] also used genetic algorithms to maximize the heat transfer performance while simultaneously minimizing the cost of materials. A set of solutions is achieved by combining these two conflicted objectives using multi-objective genetic algorithms. Genetic algorithms have been proven to be an effective and accurate way for such optimization problems. In the study upon which this thesis reports, a multi-objective genetic algorithm is used.

Effect of Local Convective Heat Transfer Coefficient on Accuracy

Fabbri [27] showed that fin profile optimization can be effective when the convective heat transfer coefficient is not too high. The local convective heat transfer

coefficient was not used in Fabbri's work, instead a constant coefficient was used. Naturally, using the local convection coefficient will make the results more accurate. Dialameh et al. [28] studied the relation between the convection heat transfer coefficient and several parameters in the cooling of fin arrays. They found that the coefficient increases when the temperature difference or fin spacing increase. They also found that it decreases as the fin length increases and that the average convection heat transfer coefficient is not sensitive to fin height and thickness. The work upon this thesis reports will take the local convective heat transfer coefficient into consideration.

CHAPTER 2
MATHMATICAL MODELING AND NUMERICAL SIMULATION

In this chapter, the problem is described then a mathematical model will be derived. The problem will be solved numerically using ANSYS FLUENT.

Problem Formulation

This is a steady-state heat transfer optimization problem. Consider a two-dimensional rectangular enclosure filled with a Newtonian fluid and having a fin on the left surface (Fig. 2-1). The length of the bottom wall is L and the length of left wall is H. To simplify the analysis, H and L will be assumed equal. Both the left and right walls are assumed isothermal. The temperature at the left wall is T_h while that at the right wall is kept $T_c (T_h > T_c)$. The top and bottom walls of the enclosure are assumed adiabatic. The fin base which is also the left side of the fin is on the left wall of the enclosure. The top and bottom sides of the fin are perpendicular to the fin base. We will only consider a rectangular fin in this work. The goal is to determine the profile and position of the fin which can provide the maximum heat transfer through the enclosure.

Gravity is taken into consideration in this natural convection process and the classical Boussinesq model is applied where the density of fluid in the buoyancy term of the momentum equations changes [29]. For a rectangular fin, the first dimensional parameter p_1 is the distance from the top of the fin to the top of the enclosure. The second dimensional parameter p_2 is the distance from top of the fin to bottom of the fin.

Mathematical Model

The dimensionless governing equations and boundary conditions will be derived in this section based on Mirehei's [15] work. This model is a steady-state heat transfer

problem so all terms in the equations are time independent. The model will not be solved analytically but instead solved numerically for the convenience of the optimization part that follows. In this steady-state problem, all time dependent derivative terms are all 0.

Conservation equation of mass of fluid:

$$\frac{\partial u}{\partial x}+\frac{\partial v}{\partial y}=0 \tag{2-1}$$

Conservation of momentum of fluid in the x direction:

$$\rho\left(u\frac{\partial u}{\partial x}+v\frac{\partial u}{\partial x}\right)=-\frac{\partial p}{\partial x}+\mu\nabla^2 u \tag{2-2}$$

Conservation of momentum of fluid in the y direction. Use $\rho(1-\beta\Delta T)$ for density in the buoyancy term based on the Boussinesq approximation [29]

$$\rho\left(u\frac{\partial v}{\partial x}+v\frac{\partial v}{\partial y}\right)=-\frac{\partial p}{\partial y}+\mu\nabla^2 v-\rho(1-\beta\Delta T)g$$

After rearranging with $\Delta T=T-\frac{T_c+T_h}{2}$

$$\rho\left(u\frac{\partial v}{\partial x}+v\frac{\partial v}{\partial y}\right)=-\frac{\partial(p+\rho g y)}{\partial y}+\mu\nabla^2 v+\rho g\beta\left(T-\frac{T_c+T_h}{2}\right) \tag{2-3}$$

Conservation of energy of the fluid:

$$u\frac{\partial T}{\partial x}+v\frac{\partial T}{\partial y}=\alpha\nabla^2 T \tag{2-4}$$

Conservation of energy of the solid:

$$\alpha_s\nabla^2 T_s=0 \tag{2-5}$$

Boundary conditions:

Non-slip condition at solid surface:

$$u=v=0 \tag{2-6}$$

Left and right wall:

$T = T_s = T_h$ at $x = 0$ (2-7)

$T = T_c$ at $x = L$ (2-8)

Top and bottom wall:

$\frac{\partial T}{\partial y} = 0$ at $y = 0\ and\ H$ (2-9)

Compatibility condition at the solid-fluid interface:

$T_s = T$ (2-10)

$q_s = q$ (2-11)

$-k\frac{\partial T}{\partial n} = -k_s\frac{\partial T_s}{\partial n}$ (2-12)

Definitions of non-dimensional variables are listed below:

$(X, Y) = \frac{(x,y)}{H}$

$(U, V) = \frac{(u,v)}{(\alpha/H)}$

$P = \left(\frac{H^2}{\rho\alpha^2}\right)(P + \rho g y)$

$\theta_s = \frac{(T_s - T_c)}{(T_h - T_c)}$

$\theta = \frac{(T - T_c)}{(T_h - T_c)}$ (2-13)

Definitions of non-dimensional parameters:

$P_1 = \frac{p_1}{H}$

$P_2 = \frac{p_2}{H}$

$S = \frac{L}{H}$

$Ra = g\beta H^3 \frac{(T_h - T_c)}{\alpha v}$

$Pr = \frac{v}{\alpha}$

$$\sigma = \frac{(\rho c)_s}{\rho c}$$

$$\kappa = \frac{k_s}{k} \quad (2\text{-}14)$$

The non-dimensional conservation equations are:

Conservation equation of mass:

$$\frac{\partial U}{\partial X} + \frac{\partial V}{\partial Y} = 0 \quad (2\text{-}15)$$

Conservation of momentum in the x direction:

$$U\frac{\partial U}{\partial X} + V\frac{\partial U}{\partial Y} = -\frac{\partial P}{\partial X} + Pr\nabla^2 U \quad (2\text{-}16)$$

Conservation of momentum in the y direction:

$$U\frac{\partial V}{\partial X} + V\frac{\partial V}{\partial Y} = -\frac{\partial P}{\partial Y} + Pr\nabla^2 V + RaPr\theta \quad (2\text{-}17)$$

Conservation of energy of the fluid:

$$U\frac{\partial \theta}{\partial X} + V\frac{\partial \theta}{\partial Y} = \nabla^2\theta \quad (2\text{-}18)$$

Conservation of energy of the solid:

$$0 = \nabla^2\theta_s \quad (2\text{-}19)$$

Non-dimensional boundary conditions are:

$$U = V = 0 \; at \; all \; solid \; surfaces \quad (2\text{-}20)$$

$$\theta = \theta_s \; = 1 at \; X = 0 \quad (2\text{-}21)$$

$$\theta = 0 \; at \; X = S \quad (2\text{-}22)$$

$$\frac{\partial \theta}{\partial Y} = \frac{\partial \theta_s}{\partial Y} = 0 \; at \;\; at \; Y = 0 \; and \; 1 \quad (2\text{-}23)$$

Non-dimensional compatibility conditions:

$$U = V = 0 \quad (2\text{-}24)$$

$$\theta = \theta_s \quad (2\text{-}25)$$

$$\frac{\partial \theta}{\partial M} = \kappa \frac{\partial \theta_s}{\partial M} \tag{2-26}$$

Numerical Simulation

From ANSYS FLUENT Theory Guide we can find FLUENT use conservation equations below in simulation [14]:

$$\frac{\partial u}{\partial x} + \frac{\partial v}{\partial y} = 0 \tag{2-27}$$

$$\rho_F \left(\frac{\partial u}{\partial t} + u\frac{\partial u}{\partial x} + v\frac{\partial u}{\partial y}\right) = -\frac{\partial p}{\partial x} + \mu_F \left(\frac{\partial^2 u}{\partial x^2} + \frac{\partial^2 u}{\partial y^2}\right) \tag{2-28}$$

$$\rho_F \left(\frac{\partial v}{\partial t} + u\frac{\partial v}{\partial x} + v\frac{\partial v}{\partial y}\right) = -\frac{\partial (p+\rho_F g y)}{\partial y} + \mu_F \left(\frac{\partial^2 v}{\partial x^2} + \frac{\partial^2 v}{\partial y^2}\right) - \rho_F \beta_F g_F \left(T - T_{ref,F}\right) \tag{2-29}$$

$$\rho_F c_F \frac{\partial T}{\partial t} + \rho_F c_F \left(u\frac{\partial T}{\partial x} + v\frac{\partial T}{\partial y}\right) = k_F \left(\frac{\partial^2 T}{\partial x^2} + \frac{\partial^2 T}{\partial y^2}\right) \tag{2-30}$$

$$(\rho c)_{s,F} \frac{\partial T}{\partial t} = k_{s,F} \left(\frac{\partial^2 T}{\partial x^2} + \frac{\partial^2 T}{\partial y^2}\right) \tag{2-31}$$

Notice $\frac{\partial u}{\partial t} = \frac{\partial v}{\partial t} = \frac{\partial T}{\partial t} = \frac{\partial T_s}{\partial t} = 0$ because of steady-state.

The coefficients and constants needed for using ANSYS FLUENT to numerically solve non-dimensional conservation equations (Equations 2-15 to 2-19 and Equations 2-27 to 2-31) were obtained by comparing the equivalent terms in the dimensional and non-dimensional conservation equations. The values and relations, that were used, are as follows:

ρ_F is set to 1, μ_F is set to Pr, β_F is set to $RaPr$, g_F is set to -1, c_F is set to 1, k_F is set to 1, $k_{s,F}$ is set to κ, $(\rho c)_{s,F}$ is set to σ.

Units of all coefficients are not changed. All values assigned are chosen arbitrarily in this optimization. When applying this optimization to certain cases which

include certain materials and certain gravity, the only change that needs to be made in these assigned values are Pr, Ra, κ and σ.

In the comparison between the y momentum conservation Equation (2-17) and Equation (2-19), $(p + \rho_F gy)$ plays the same role of P as the total pressure. The value 0 is chosen for $T_{ref,F}$ to make the comparison easier since $T_{ref,F}$ will not affect the problem which is in steady-state [15, 31].

The value of gravity is positive when the direction of gravity is upward, which is the same direction of the y axis. If the direction of gravity is downward, the value of gravity is negative.

In the numerical simulation, the following parameters are set as below:

$Pr = 1$, $Ra = 10^7$, $\kappa = 1$, $\sigma = 10$.

The dimensionless temperature is set as follows: $\theta = 1\ at\ X = 0$, $\theta = 0\ at\ X = S$. To avoid ANSYS error when θ is set to 0 at the boundary because the unit of temperature is Kelvin, we keep the difference of θ between $X = 0$ and $X = 1$. Solid area fraction of the enclosure is 16%. Mesh elements are uniform and mesh size is set to 0.004. The “SIMPLEC” algorithm is chosen as the pressure-velocity coupling scheme [15].

The average heat flux at the right wall is defined as:

$$\langle \mathrm{q}'' \rangle_{x=L} = \frac{1}{H}\int_0^H (-k\frac{\partial \mathrm{T}}{\partial \mathrm{x}}\Big|_{\mathrm{x=L}})dy \tag{2-32}$$

The corresponding non-dimensional average heat flux at the right wall is defined as:

$$Q_c'' = \langle \mathrm{q}'' \rangle_{x=L} / [kH(T_h - T_c)/L] = \frac{1}{S}\int_0^S (-\frac{\partial \theta}{\partial \mathrm{X}}\Big|_{\mathrm{X=S}})dY \tag{2-33}$$

The value of non-dimensional heat flux at the right wall is equal to the non-dimensional average heat flux at the right wall in this case because $S = 1$ is assumed.

$$Q_c = SQ_c'' \tag{2-34}$$

In the optimization section, multiple objectives genetic algorithm (MOGA) is chosen as the optimization method. The number of initial samples is 100. The number of samples per iteration is set to 100. The number of samples in each iteration will affect the optimization process and sometimes determines if the optimization will converge. If the number per iteration is too small there will not be enough chromosomes for achieving the final results. Sometimes it may still get the right results but most likely the optimization would converge to a local maximum due to the lack of good samples. However, the process will be slower as the number per iteration increases. It will take longer time for one generation to produce the next generation. The proper number of samples per iteration should be pre-selected. A value of 100 is recommended by FLUENT. The convergence Stability Percentage is set to 2%. The Convergence Stability Percentage criterion looks for population stability, based on the mean and standard deviation of the output parameters. When a population is stable with regards to the previous one, the optimization is converged. If the Convergence Stability Percentage is set too high, the samples will be considered converged too fast when they still have some potential to evolve. If the Convergence Stability Percentage is set lower, the optimization results will be more accurate and at the same time will take more time. If it is set to 0, all samples will be the same in the last iteration. A value of 0 is the best value for the Convergence Stability Percentage but 2% is recommended for saving time and several candidates for samples will be selected. The Mutation probability is set

to 1%. The Crossover probability is set 98%. Mutation is the reason the optimization process can keep moving. Some good genes that do not exist now can only be created by mutation. As the mutation probability increases the optimization will be more random. Therefore, low mutation probability is recommended but it cannot be set to 0. Low crossover probability will make the generation more stable and will get the results faster but less accurate. High crossover probability (>0.9) is also recommended [30].

For a rectangular fin, the first parameter P_1 is the non-dimensional distance from top of the fin to top of the enclosure. The second parameter P_2 is the non-dimensional distance from top of the fin to bottom of the fin. To avoid incompatible errors in ANSYS FLUENT, the upper limit of both parameters is set to 0.995 and lower limit is set to 0.005 to make sure the parameters are greater than the minimum mesh size.

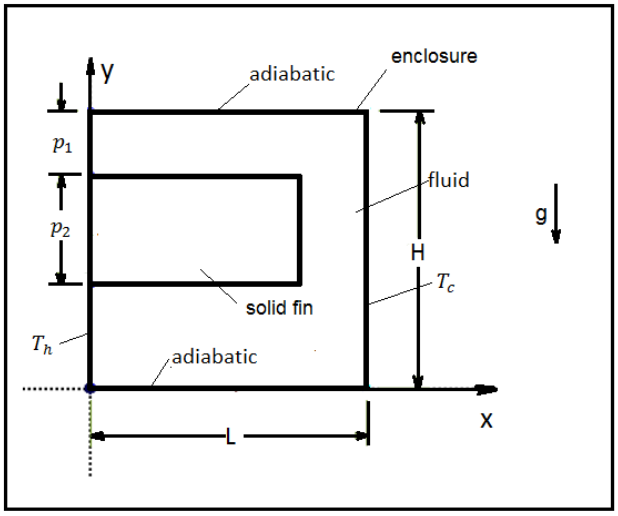

Figure 2-1. Schematic of the enclosure

CHAPTER 3
RESULTS AND DISCUSSIONS

The optimal parameters are $P_1 = 0.41361$ and $P_2 = 0.16749$. The non-dimensional maximum heat flux at the right wall is 14.822.

In this chapter, sensitivity analysis will be done on P_1 and P_2 to observe their effect on the total heat flux. The effects from these two different parameters will be compared.

The optimized fin profile and position will be shown as well as the temperature and streamline distribution of the optimal case.

A mesh test is performed to ensure the accuracy of the results.

Sensitivity Analysis of P_1 and P_2 with Total Heat Flux

Effect of P_1 on non-dimensional heat flux at right wall

The effect of P_1 on the non-dimensional heat flux at values of $P_2 = 0.16$, $P_2 = 0.20$, $P_2 = 0.30$, $P_2 = 0.40$, $P_2 = 0.50$ is shown in Figure 3-1. When P_2 is fixed at a certain value, the effect of P_1 on non-dimensional heat flux at the right wall can be observed. As the value of P_1 increase, the non-dimensional heat flux at the right wall will decrease at $P_2 = 0.20$, $P_2 = 0.30$, $P_2 = 0.40$, $P_2 = 0.50$. When $P_2 = 0.16$, as P_1 increases, the non-dimensional heat flux at the right wall will also increase and will reach its maximum near $P_1 = 0.45$. Then the non-dimensional heat flux at the right wall will drop. This trend is observed for all other curves.

Comparing results from the different value of P_2, the non-dimensional heat flux at the right wall is found to be higher at smaller values of P_2.

Effect of P_2 on non-dimensional heat flux at right wall

The effect of P_2 on the non-dimensional heat flux at $P_1 = 0.10$, $P_1 = 0.20$, $P_1 = 0.30$, $P_1 = 0.40$, $P_1 = 0.50$ is shown in Figure 3-2. As P_2 increase the non-dimensional heat flux at the right wall will also decrease. P_1 and P_2 have the same trend when affecting the non-dimensional heat flux at the right wall. However, P_2 seems to have greater effect than P_1 on the non-dimensional heat flux at the right wall. P_1 and P_2 are independent parameters but notice that P_1 cannot be any value between its upper and lower limit for a specific P_2. The upper and lower limits are overall limits for parameters. There is a certain limit for P_1 at each P_2 value.

Optimal Profile and Position of Rectangular Fin and Optimized Heat Flux at the Right Wall

Considering the parameters and objectives in the numerical simulation part, multi- objective genetic algorithm (MOGA) is selected as the optimization method. Instead of considering the non-dimensional area of the fin being 0.16 as an object, we will consider it as a constraint to make the optimization process faster. To achieve this, the fin length and height are set as two dependent parameters to make sure the area of the fin is 0.16 and one of them is suppressed to avoid unnecessary work for ANSYS.

The model is simulated using the following parameters: $Pr = 1$,$Ra = 10^7$,$\kappa = 1$,$\sigma = 10$.

After optimization $P_1 = 0.41361$ and $P_2 = 0.16749$. The maximum heat flux at the right wall is 14.8.

Analysis of Isotherm Contour and Streamline Contour

Figure 3-3 shows the optimized profile and position for the rectangular fin along with the distribution of the isotherms inside the enclosure. Figure 3-4 shows the distribution of the streamlines for this case.

The gradient of temperature is high near the hot and cold wall. The isotherms are perpendicular to the top and bottom wall because the top and bottom walls of the enclosure are adiabatic and the temperature change of the fluid in the middle part of the enclosure is smoother than that near the hot and cold walls. For the fluid near the hot and cold walls, the temperature gradient is higher than that of the solid fin because of convection. However, conduction in the solid makes the temperature gradient higher than that in the fluid which is not near the hot and cold walls where convection is low. The fin divides the fluid geometrically into a higher part and a lower part. For the fluid above the fin, the cold fluid is first heated at the bottom left corner of this part by both the hot wall and the fin. Then it goes up to the top wall because buoyancy and gravity are both taken into consideration and the density of fluid decreases as the temperature increase. The top wall is adiabatic so no heat from the fluid will dissipate through the wall. The stream will only be cooled by the cold fluid below it which will result in small temperature gradients and horizontal isotherms in the middle of this part of the enclosure. After moving right to the cold wall, the stream will dissipate heat quickly and the fluid become denser. Then most of the fluid cooled by the cold wall will go downward to the fin which has a higher temperature because of conduction. The fluid stream is heated by the fin again while migrating left until it returns to the bottom left corner of this part of the enclosure. A similar process will occur in the part of the enclosure below the fin.

Mesh test

The optimization is performed at a mesh size of 0.004. To ensure the result is independent from the mesh size, a finer mesh is applied to the same optimization process. The new mesh size is 0.002 which is half of the former one. The optimal case is at: $P_1 = 0.3915$ and $P_2 = 0.1700$. The maximum heat flux at the right wall is 14.3. Deviation of all parameters and maximum heat flux at the right wall from the former results is less than 5%. We believe that the optimization process as well as the results generated are fairly independent when the mesh size is 0.004.

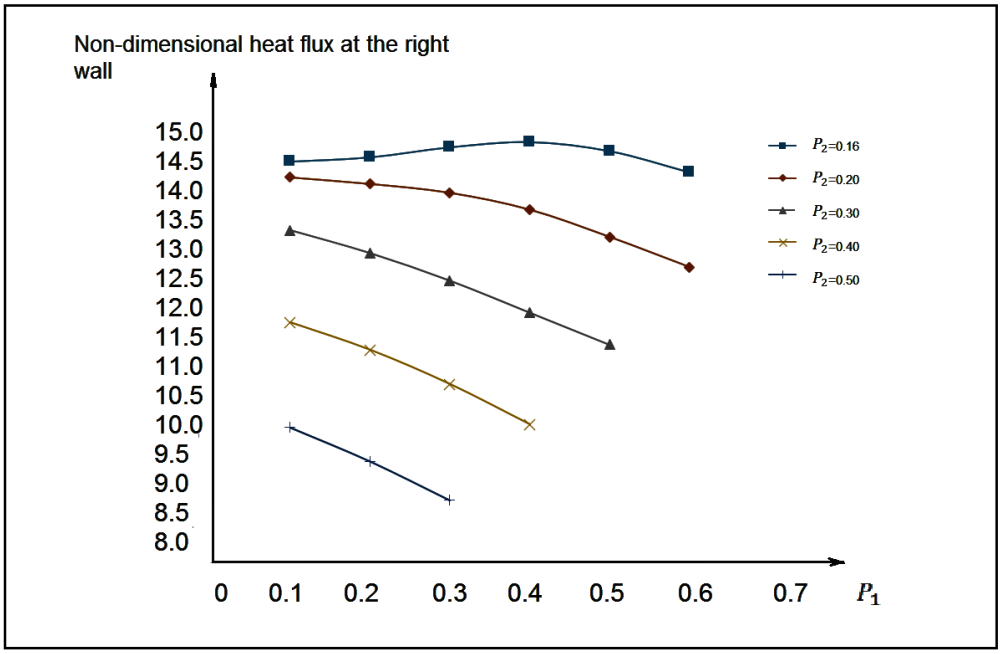

Figure 3-1. Effect of P_1 on the non-dimensional heat flux at right wall at $P_2 = 0.16$, $P_2 = 0.20$, $P_2 = 0.30$, $P_2 = 0.40$, $P_2 = 0.50$

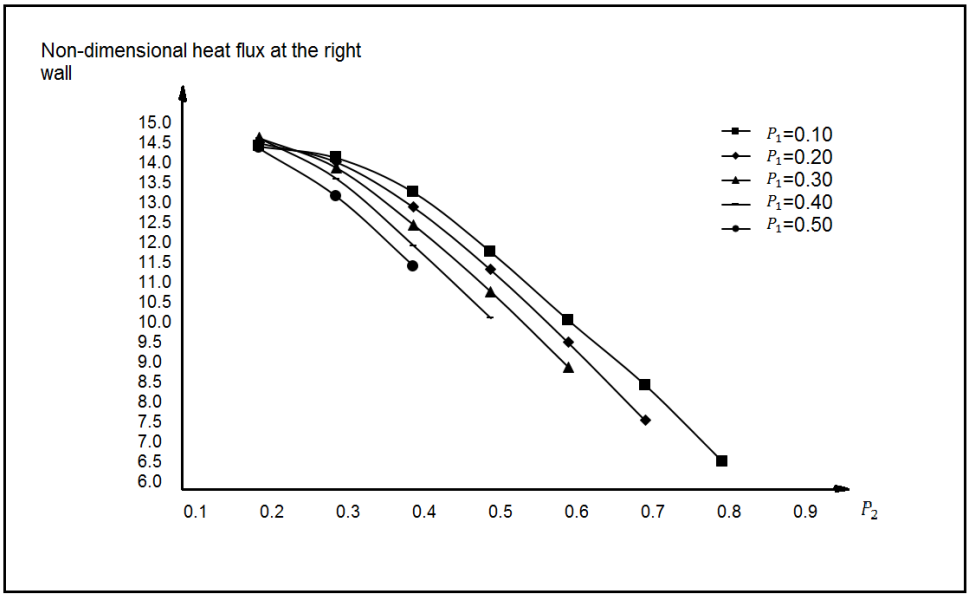

Figure 3-2. Effect of P_2 on the non-dimensional heat flux at right wall at $P_1 = 0.10$, $P_1 = 0.20$, $P_1 = 0.30$, $P_1 = 0.40$, $P_1 = 0.50$

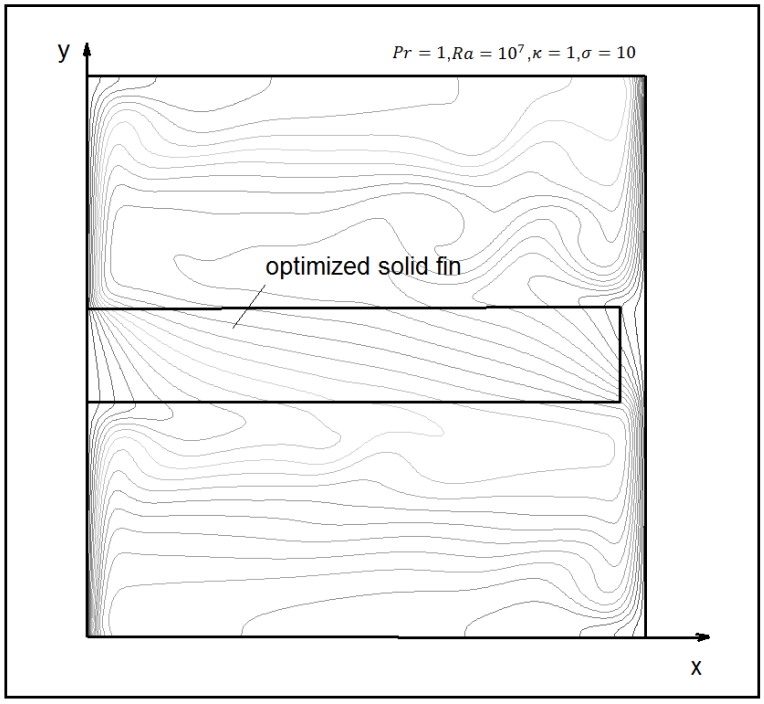

Figure 3-3. Shots of isotherm distributions of enclosure for optimized rectangular fin, steady state,$Pr = 1, Ra = 10^7, \kappa = 1, \sigma = 10$.

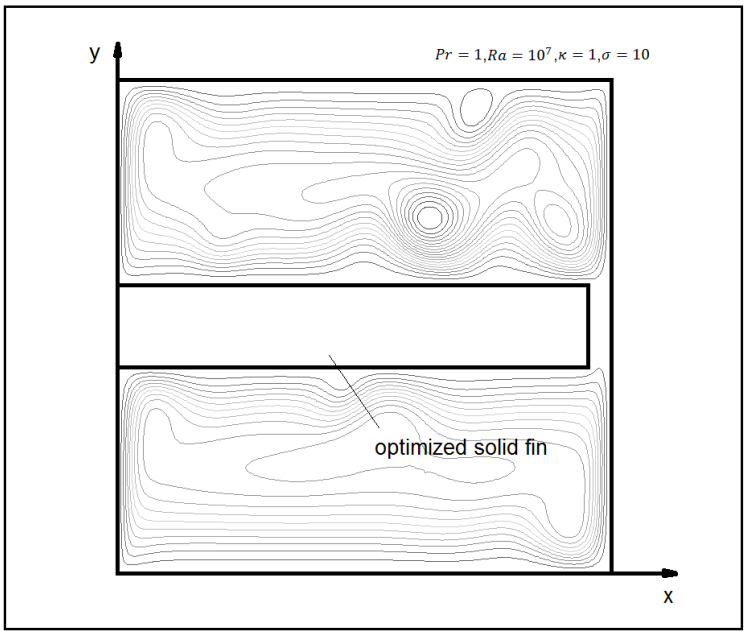

Figure 3-4. Shots of streamlines of enclosure for optimized rectangular fin, steady state, $Pr = 1, Ra = 10^7, \kappa = 1, \sigma = 10$.

CHAPTER 4
CONCLUSIONS AND RECOMMENDATIONS

Conclusions

In this thesis, a rectangular fin based on a hot plate inside an enclosure is optimized to its optimal geometry and position to get the maximum heat transfer. Gravity and two-dimensional heat transfer and the local convective heat transfer coefficient are all accounted for. Since the heat transfer performance improves as the fin area increases, which results in more cost for the fin material, the area of the fin is kept at 0.16. An optimal case is obtained through the use of genetic algorithms. All variables are non-dimensionalized for future design when it comes to different materials and different enclosure geometries. The values of $Pr = 1$ and $Ra = 10^7$ will be set at this optimization. The optimal parameters are $P_1 = 0.41361$ and $P_2 = 0.16749$. The non-dimensional maximum heat flux at right wall is 14.822.

Recommendations

The current study pertains to optimization for only one fin. Fin arrays are proven to be more effective than single fins and we can still use genetic algorithms to get the optimal number of fins and optimal geometries for fin arrays.

Also, the area of the fin was kept constant in the current study. However this area may not be the optimal area which can produce the best ratio of cost and heat transfer performance. If the area as along with heat transfer were allowed to change in a multi-objective genetic algorithm, a wider set of optimal cases could be achieved.

Also, three-dimension analysis will be more applicable in electronic cooling and other industries.

In the current study, gravity is incorporated in the analysis through the Rayleigh number. This can be expanded in a future investigation. This will make it easier to perform such optimization when solving problems related to space where gravity is different from that on the surface of the earth.

LIST OF REFERENCES

[1] Merrikh, A. A., and J. L. Lage. “From continuum to porous-continuum: the visual resolution impact on modeling natural convection in heterogeneous media." D.B. Ingham, I. Pop (Eds.), Transport Phenomena in Porous Media, Chapter 3, Elsevier Science, England (2005).

[2] Merrikh, A. A., and J. L. Lage. "Natural convection in nonhomogeneous heat-generating media: Comparison of continuum and porous-continuum models." Journal of Porous Media 8.2 (2005): 149-163

[3] Whitaker, S. "Theory and applications of transport in porous media: The method of volume averaging." Kluwer Academic Publishers, The Netherlands (1999)

[4] Merrikh, A. A. "Blockage effects in natural convection in differentially heated enclosures." Journal of Enhanced Heat Transfer 8.1 (2001): 55-72

[5] Merrikh, A. A., and J. L. Lage. "Natural convection in an enclosure with disconnected and conducting solid blocks." International Journal of Heat and Mass Transfer 48.7 (2005): 1361-1372.

[6] Massarotti, N., P. Nithiarasu, and A. Carotenuto. "Microscopic and macroscopic approach for natural convection in enclosures filled with fluid saturated porous medium." International Journal of Numerical Methods for Heat & Fluid Flow 13.7 (2003): 862-886.

[7] Braga, Edimilson J., and Marcelo JS De Lemos. "Heat transfer in enclosures having a fixed amount of solid material simulated with heterogeneous and homogeneous models." International Journal of Heat and Mass Transfer 48.23 (2005): 4748-4765.

[8] Braga, Edimilson J., and Marcelo JS de Lemos. "Laminar natural convection in cavities filled with circular and square rods." International Communications in Heat and Mass Transfer 32.10 (2005): 1289-1297.

[9] Pourshaghaghy, A. Hakkaki-Fard, A. and Mahdavi-Nejad A., “Direct simulation of natural convection in square porous enclosure”, Energy Conversion and Management 48.5 (2007): 1579-1589.

[10] Jamalud-Din, S. D., Rees, D. A. S., Reddy, B. V. K., and Narasimhan, A.. Prediction of natural convection flow using network model and numerical simulations inside enclosure with distributed solid blocks. Heat and Mass Transfer 46.3 (2010): 333-343.

[11] Narasimhan, Arunn, and B. V. K. Reddy. "Natural convection inside a bidisperse porous medium enclosure." Journal of Heat Transfer 132.1 (2010): #012502.

[12] Junqueira, S. L., De Lai, F. C., Franco, A. T., and Lage, J. L. "Numerical investigation of natural convection in heterogeneous rectangular enclosures." Heat Transfer Engineering 34.5-6 (2013): 460-469.

[13] Qiu, H., Lage, J. L., Junqueira, S. L., and Franco, A. T. “Predicting the nusselt number of heterogeneous (porous) enclosures using a generic form of the berkovsky–polevikov correlations.” Journal of Heat Transfer 135.8 (2013): #082601.

[14] Mirehei, S. M., Franco, A. T., Junqueira, S. L. M., and Lage, J. L. “Periodic Horizontal Heating of Enclosed Disconnected Solid Bodies Saturated With a Fluid. In ASME 2014 International Mechanical Engineering Congress and Exposition (2014): V08AT10A034.

[15] Mirehei, S. M. “Simulations and analyses of natural convection inside heterogeneous containers heated by solar radiation” Diss. Southern Methodist University (2015).

[16] Huang, Guei-Jang, and Shwin-Chung Wong. "Dynamic characteristics of natural convection from horizontal rectangular fin arrays." Applied Thermal Engineering 42 (2012): 81-89.

[17] Harahap, Filino, Herry Lesmana, and IKT Arya Sume Dirgayasa. "Measurements of heat dissipation from miniaturized vertical rectangular fin arrays under dominant natural convection conditions." Heat and Mass Transfer 42.11 (2006): 1025-1036.

[18] Al-Doori, W. H. A. R. "Enhancement of natural convection heat transfer from the rectangular fins by circular perforations." International Journal of Automotive and Mechanical Engineering 4 (2011): 428-436.

[19] Dannelley, Daniel. “Enhancement of extended surface heat transfer using fractal-like geometries.” Diss. University of Alabama (2013).

[20] Azarkish, H., S. M. H. Sarvari, and A. Behzadmehr. "Optimum design of a longitudinal fin array with convection and radiation heat transfer using a genetic algorithm." International Journal of Thermal Sciences 49.11 (2010): 2222-2229.

[21] Bobaru, Florin, and Srinivas Rachakonda. "Optimal shape profiles for cooling fins of high and low conductivity." International Journal of Heat and Mass Transfer 47.23 (2004): 4953-4966.

[22] Kang, Hyung Suk, and Dwight C. Look Jr. "Optimization of a trapezoidal profile annular fin." Heat Transfer Engineering 30.5 (2009): 359-367.

[23] Hamadneh, N., Khan, W. A., Sathasivam, S., and Ong, H. C. "Design optimization of pin fin geometry using particle swarm optimization algorithm." PloS one 8.5 (2013): e66080.

[24] Hajabdollahi, F., Rafsanjani, H. H., Hajabdollahi, Z., and Hamidi, Y. “Multi-objective optimization of pin fin to determine the optimal fin geometry using genetic algorithm.” Applied Mathematical Modelling, 36.1 (2012): 244-254.

[25] Wang, Jiansheng, and Xiao Wang. "The heat transfer optimization of conical fin by shape modification." Chinese Journal of Chemical Engineering 24.8 (2016): 972-978.

[26] Najafi, Hamidreza, Behzad Najafi, and Pooya Hoseinpoori. "Energy and cost optimization of a plate and fin heat exchanger using genetic algorithm." Applied Thermal Engineering 31.10 (2011): 1839-1847.

[27] Fabbri, Giampietro. "A genetic algorithm for fin profile optimization." International Journal of Heat and Mass Transfer 40.9 (1997): 2165-2172.

[28] Dialameh, L., M. Yaghoubi, and O. Abouali. "Natural convection from an array of horizontal rectangular thick fins with short length." Applied Thermal Engineering 28.17 (2008): 2371-2379.

[29] Tritton, D. J. “Physical Fluid Dynamics” Von Nostrand Reinhold, New York (1979).

[30] Fluent, Ansys. "12.0 Theory Guide." Ansys Inc 5 (2009).

[31] Mirehei, S. M., and J. L. Lage. "Periodic natural convection inside a fluid saturated porous medium made of disconnected solid obstacles: A continuum approach." ASME 2016 Heat Transfer Summer Conference. 7. (2016)

BIOGRAPHICAL SKETCH

Miao Huang received his master's degree from University of Florida in the fall of 2017. He received his bachelor's degree from Southeast University in the spring of 2015.